AIAA JOURNAL
Vol. 35, No. 8, August 1997

Quantitative Density Measurements by Rayleigh Scattering Behind a Plane Turbine Cascade

K. Fiedler,* O. Sieber,† and C. Jakiel‡
Universität der Bundeswehr Hamburg, D-22043 Hamburg, Germany

An optical density measuring system based on Rayleigh scattering was installed at an atmospheric wind tunnel. The system monitors the scattered light induced by a laser sheet irradiating the flowfield behind a plane VKI-1 turbine cascade. Because of the scattering of air molecules, tracer particles are not required. The measuring procedure is based on a relative measurement and needs no calibration except consideration of the incident laser light energy. The system allows quantitative recording of the two-dimensional density field in a very short time. The density distributions behind the VKI-1 cascade are presented as experimental results for subsonic and transonic flow. The experimental data are compared with the results of a two-dimensional Navier–Stokes calculation. The results indicate that the measurement of the whole three-dimensional flowfield in and behind cascades is possible if the experimental arrangement is adjusted.

Introduction

THE application of cascade flow simulation methods represents an important instrument for designing efficient turbomachinery components. In the development of such a simulation program, blade pressure distributions together with the corresponding surface Mach number distributions are used for validating the numerical results. Qualitative measurements, such as schlieren pictures, are taken into consideration as well. Because of an increasing need for flow simulation under real conditions, i.e., as a three-dimensional, compressible, viscid, turbulent, and possibly shock-wave-affected flow, the expectations on measurements and calculations are also increasing. Therefore, additional information is needed, e.g., on the blade boundary-layer design or on the mixing process between jet and wake. At this point, conventional measuring systems usually have limits. The measurements of pneumatic probes, for example, are often not precise enough because of their flow displacement, especially close to surfaces and in supersonic flow. Inasmuch as the resolution of conventional systems, in general, is low, more and more optical measuring systems are applied.

Because until now the experimental results of the two-dimensional flowfield behind cascades did not offer sufficient information in all cases, a measurement system was installed at the Laboratory for Turbomachinery at the Universität der Bundeswehr Hamburg to get more quantitative information in this area. For this, the Rayleigh scattering measuring technique was selected because as an optical system it offers additional advantages. This measuring system needs no tracer particles, and it yields the quantitative information of density. The Rayleigh scattering technique is well proven and is applied for acquiring fluid mechanics information, e.g., to measure the concentration field of a turbulent gas jet,[1] to obtain quantitative information on shock wave/boundary-layer interaction,[2,3] or to get information about the turbulent nature of the flow.[4] This paper describes the installed measuring system and the corresponding measuring procedure. Results from the area behind a turbine cascade are presented and compared with numerical results.

Experiments

The air for the laboratory atmospheric wind tunnel (Fig. 1) is supplied by a centrifugal compressor. If pressure ratios higher than 2.0 or mass flows greater than 18 kg/s are required, a second compressor is also used. Prior to entering the compressors, the ambient air passes through a dust filter. The total temperature of the compressed air can be kept constant by water cooling. This air supply design allows steady-state testing of subsonic and supersonic flow in the wind tunnel without time limits. After entering the moderation chamber, where the total temperature, the total pressure, and the humidity are measured, the air is led to the test section. The blades are mounted in the test section with fixed geometrical parameters in a changing frame forming the endwalls of the flow channel and considering measuring apertures. The frame is attached to a slewable rig for adjusting the inlet angle. For the measurements, the dimensions of the inlet flow channel were 300×100 mm, allowing the installation of a cascade of 12 blades.

The cascade used is of the type VKI-1 (Fig. 2), which is typical for a coolable gas turbine rotor blade section designed for transonic flow. It was proposed for comparisons of experimental and computational results by the von Kármán Institute (VKI) in 1973.[5] Since then it has been investigated intensively by experiments as well as flow calculations.

An excimer laser (Lambda-Physik LPX 110i) modified with a polarizer is employed as the light source. This ArF laser works in the deep uv at 193 nm. The emitted Rayleigh light is imaged by an intensified charge-coupled device (CCD) camera (LaVision) via a uv-light-sensitive lens (UV-Nikkor 105 mm, f/4.5).

The CCD chip has a resolution of 384×286 pixels, 12-bit per pixel. A 486 personal computer with special software (LaVision) controls the laser and the imaging system. The evaluation of the acquired CCD images is also possible with this software.

The arrangement used for beam positioning is shown in Fig. 3. The laser beam is blanked out by a double aperture directly after emerging. With the help of three mirrors, the beam is positioned in the direction parallel to the endwalls and parallel to the trailing-edge plane. The mirror arrangement allows varying the distance of the laser beam to the trailing edges and the position between the endwalls. For the measurements presented, the beam position between the endwalls was fixed at 50% of the test section width. Two cylinder lenses focus the laser beam to reduce the thickness under 0.5 mm at a width of about 20 mm. At these dimensions the area of measurement can be considered as a plane. At least one adjustable aperture is mounted to suppress direct irradiation of the trailing edges and to fix the sheet cross section as a rectangle.

To get precise monitoring of the beam energy, some laser light is cut off at the third mirror and, after transformation to longer wavelength, led through a liquid light guide. The transformation is necessary because the lightwave guide is only transparent for wavelengths longer than $\lambda = 260$ nm. The second exit of the light pipe is fixed at the endwall opposite to the measuring window, and so the one camera can image the transmitted energy signal while taking the images (Fig. 4). It was proved by experiments that the recorded

Received June 14, 1996; revision received March 11, 1997; accepted for publication April 25, 1997.

*Professor, Department of Mechanical Engineering, Holstenhofweg 85.
†Assistant Professor, Department of Mechanical Engineering, Holstenhofweg 85.
‡Assistant Scientist, Department of Mechanical Engineering, Holstenhofweg 85.

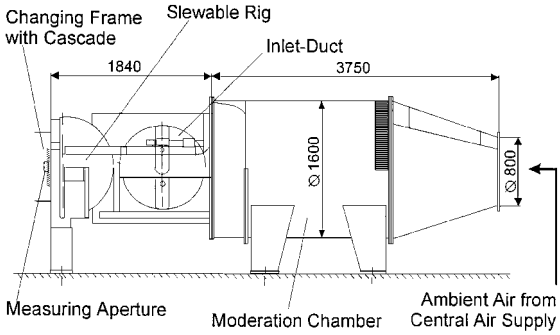

Fig. 1 Wind tunnel for straight cascades.

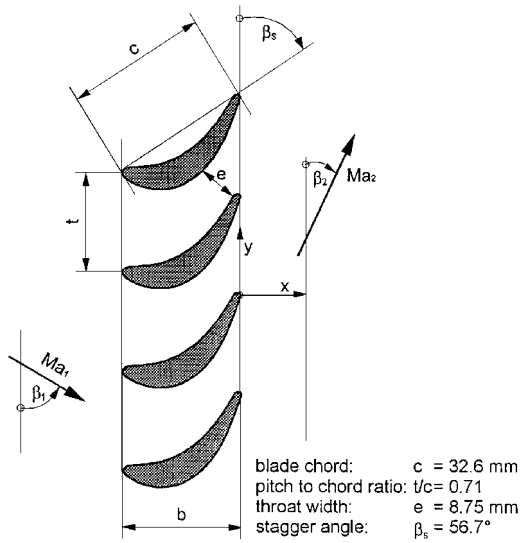

Fig. 2 VKI-1 cascade geometry.

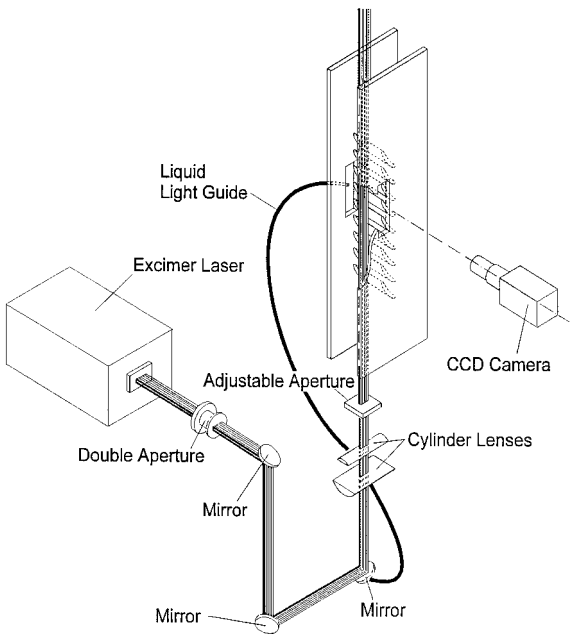

Fig. 3 Experimental setup.

energy signals show a linear dependence on the laser output energy within the range of possible beam energy fluctuations of maximum ±5% from pulse to pulse.[6]

Because no open apertures are allowed, in order to properly guide the flow, the Rayleigh scattered light reaches the camera through a silica glass window with optimized transmission rate of 193 nm. The material for the background insert was selected to minimize direct reflections of scattered light to the camera. We found the same silica glass very suitable because no significant differences of the intensities were detected with the window being built in or not. To reduce the influence of light scattered outside the test section, the laser beam was covered as far as possible.

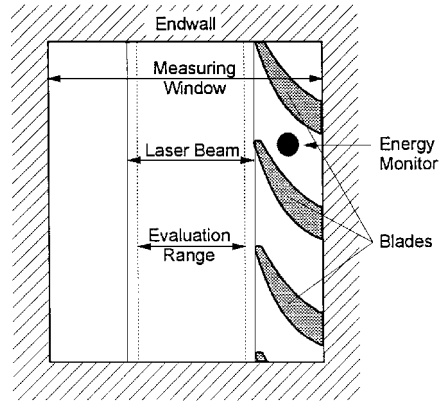

Fig. 4 Measuring area.

Rayleigh Scattering

The phenomenon of Rayleigh scattering belongs to the group of elastic scattering processes. This means that Rayleigh scattering is a process without a permanent exchange of energy between light and matter but with change in the light direction. According to Planck's law, the frequency of the scattered light is equal to the frequency of the incident light.

The intensity of Rayleigh scattered light can be described by a fundamental correlation if the following simplifications are assumed.

1) The gas atoms and gas molecules are considered as dielectric spheres with a diameter that is smaller than the wavelength of the incident light. Therefore, the electric field can be regarded as constant over the sphere.

2) The test section is irradiated in one direction with monochromatic and linearly polarized light. The scattered light is linearly polarized as well.

3) The particles are randomly spread in the measuring volume.

4) Multiple scattering is neglected, i.e., light that has been scattered at one particle will not be scattered at another particle.

With these assumptions, the Rayleigh scattering intensity of all air molecules in the measuring volume is obtained by

$$I = \sigma \bar{N} I_0 / r^2 \tag{1}$$

Thus, the intensity of the detected light I depends on the effective scattering cross section σ, the number of particles N, the distance from the measuring volume r, and the intensity of the incident laser light I_0 (Ref. 6). The scattering cross section is the theoretical effective plane for the incident photons. This plane is not equal to the geometrical cross section. The effective cross section is highly dependent on the frequency of the incident radiation and on the characteristics of the particles. Although σ of air depends on pressure, temperature, and composition of air,[7] the effective cross section can be assumed to be constant for the conditions being found in this atmospheric wind tunnel.[6] It is obvious that the constant composition of air in the test section is a basic requirement.

Measurement Procedure

The imaged signal for each pixel $S(x, y)$ can be described by

$$S(x, y) = c(x, y) I_0(x, y) \sigma \bar{N}(x, y) \tag{2}$$

with the constant value c, which contains all spatially dependent but constant parameters such as distance from the measuring plane and the setting of the optical equipment and the software. Equation (2) does not contain the share of possible stray light because it can be assumed to be small compared to the Rayleigh signal. This assumption is legitimate because scattered light reflected at the background plane could be minimized (see preceding section) and no significant stray light from other surfaces, e.g., the blades, could be detected. Because the laser light intensity and the composition of the air is considered as staying constant and the number of molecules $\bar{N}(x, y)$ is proportional to the density $\rho(x, y)$, Eq. (2) can be rewritten as

$$S(x, y) = K(x, y) \rho(x, y) \tag{3}$$

The evaluation of Rayleigh scattering can only be based on a relative measurement because the effect of the real density variations

is smaller than the also detected aberrations such as laser beam inhomogenities and the spatially dependent sensitivity of the imaging optics. Therefore, first a wind-on image is taken, i.e., during wind-tunnel operation. The measured signal contains the information on density variation given by

$$S_1(x, y) = K(x, y)\rho_1(x, y) \tag{4}$$

Additionally, a wind-off image is taken under standard conditions, i.e., across the whole field of view, the density has to be on the same level and exactly known:

$$S_0(x, y) = K(x, y)\rho_0 \tag{5}$$

The air filling the test section during wind-off imaging has passed through the same way as the air at wind-on imaging. Because of this, the composition of air is the same and the use of the factor $K(x, y)$ in both relations (4) and (5) is legitimate. The pixelwise division of the two signals yields a ratio for each pixel that is proportional to the local density in the flowfield,

$$F_1(x, y) = \frac{S_1(x, y)}{S_0(x, y)} = \frac{\rho_1(x, y)}{\rho_0} \tag{6}$$

After this, the density field is determined qualitatively. With this kind of evaluation, the potential sources of errors, such as the aforementioned beam aberrations or the optical setup, are eliminated if they are stationary and on the same level in both pictures.

In Fig. 4, a taken image is shown schematically. The measurement window is positioned in the endwall to allow a view into the measuring volume and the nearby trailing edges of the blades. The laser beam radiates through the measuring volume parallel to the trailing edges. Because the laser intensities decline rapidly at the lateral borders of the beam, the signal-to-noise ratio is too low in these areas. Thus, the evaluation range is smaller than the width of the laser beam.

The aforementioned easy measurement procedure (6) presupposes identical laser light energy I_0 while taking the wind-on and the wind-off image. If this cannot be achieved, the energy level has to be known exactly to be able to calibrate the density ratio $F_1(x, y)$. Because the beam energy fluctuates from pulse to pulse and decreases during the operation due to limited lifetime of the laser gases, an energy monitor is used as described earlier. Because the energy monitor output is part of the recorded image (Fig. 4), an average value of the energy monitor signal is calculated from both the wind-on image ($\varnothing EM_1$) and the wind-off image ($\varnothing EM_0$). Now calibration of the density ratio $F_1(x, y)$ is possible:

$$F_{1,c(x,y)} = F_1(x, y)(\varnothing EM_0/\varnothing EM_1) \tag{7}$$

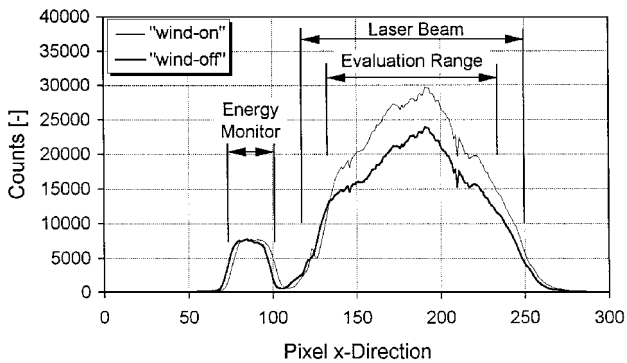

Fig. 5 Intensity distribution in *x* direction.

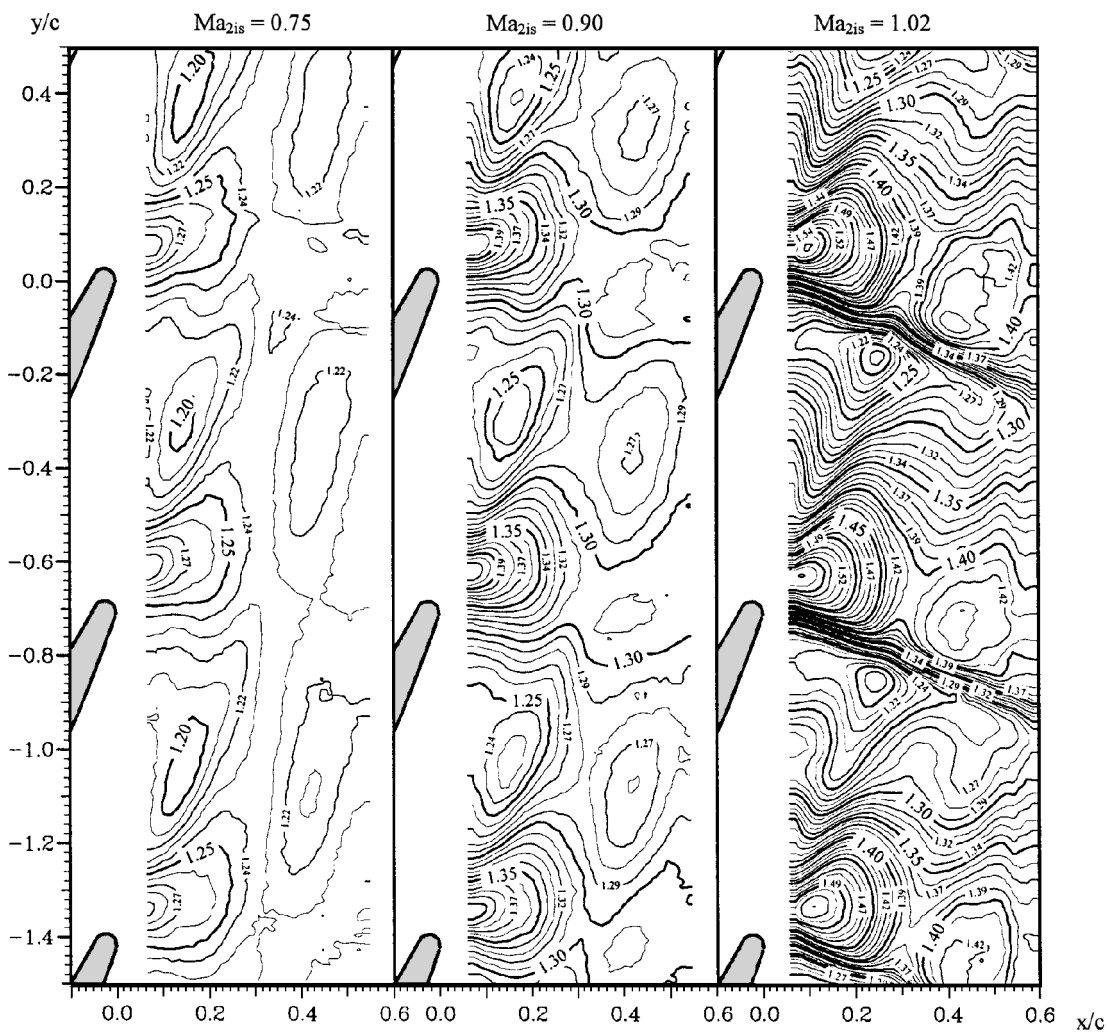

Fig. 6 Measured density fields.

Without taking the laser energy into consideration, the average values of the density ratio deviate up to 6% from their mean value although they were measured at the same flow conditions. But with energy monitor calibration the deviation can be reduced to less than 1%. This calibration has no influence on the qualitative result because the whole density field is converted with a constant ratio. Usually the ratio $\varnothing^{EM_0}/\varnothing^{EM_1}$ varies from 0.94 to 1.02.

Figure 5 shows a typical intensity profile of the measuring volume and the energy monitor. The differences of density between the wind-on and wind-off image can be seen as distances between the two profiles in the range of the laser beam. Likewise, these two profiles with similar behavior elucidate the necessity of a relative measurement, inasmuch as the intensity differences caused by the density variation are smaller than the differences caused by the beam inhomogenities. The irregularities at pixels 140 and 210 may be attributed to CCD chip errors. These errors will be eliminated by the division of the images. The intensities in the area of the energy monitor are roughly three times inferior to the Rayleigh scattering intensities, but they are even more than one order of magnitude higher than the signals from the areas not being evaluated. Thus, a clear distinction of the areas is possible. In Fig. 5 the shifting of the energy monitor range also can be seen. This is caused by motion of the cascade because the fixed lightguide outlet moves together with the cascade during wind-tunnel operation at high pressures. The shifting is very small (< 1 mm) and considered at the calculation of $\varnothing^{EM_0}$ and $\varnothing^{EM_1}$.

Simultaneously with recording the wind-off image, the pressure and the temperature in the room are measured for calculating the density ρ_0, which is constant across the whole field of view. With this, the density field at wind-tunnel operation is determined qualitatively and quantitatively:

$$\rho_1(x, y) = F_{1,c}(x, y)\rho_0 \tag{8}$$

In these experiments, altogether 2500 laser shots were summed up for both wind-on and wind-off images. This number basically is yielded from 50 shots summed up on chip. The intensities of 10 of these bursts were read out, added by the software, and stored on a hard disk. This process is completed five times without breaks. The result of averaging these five data sets is the information of the density field. A statistical evaluation of the five single sets increases the opportunity of detecting errors such as unusual laser energy fluctuations or Mie particles. With this measurement procedure, it is also proved that photon shot noise is not the limiting factor for density accuracy.

The position of the laser beam relative to the blades and the extension of the evaluation range both were determined with optical aids. The uncertainty of position and extension is lower than 1.5% according to the pitch.

The given setup allows the measurement of the density behind three flow channels at the same time with a resolution of 35 pixel/mm^2. A second setup was tested with roughly half the distance between measuring plane and objective, i.e., with four times higher optical resolution. No resulting additional information could be received from the density fields, but it had to be compensated for the disadvantage of receiving measurements of less than two flow channels.

Because of the use of an atmospheric wind tunnel, the possibility of water condensation and dust particles in the utilized air has to be taken into consideration. Condensation can occur at high

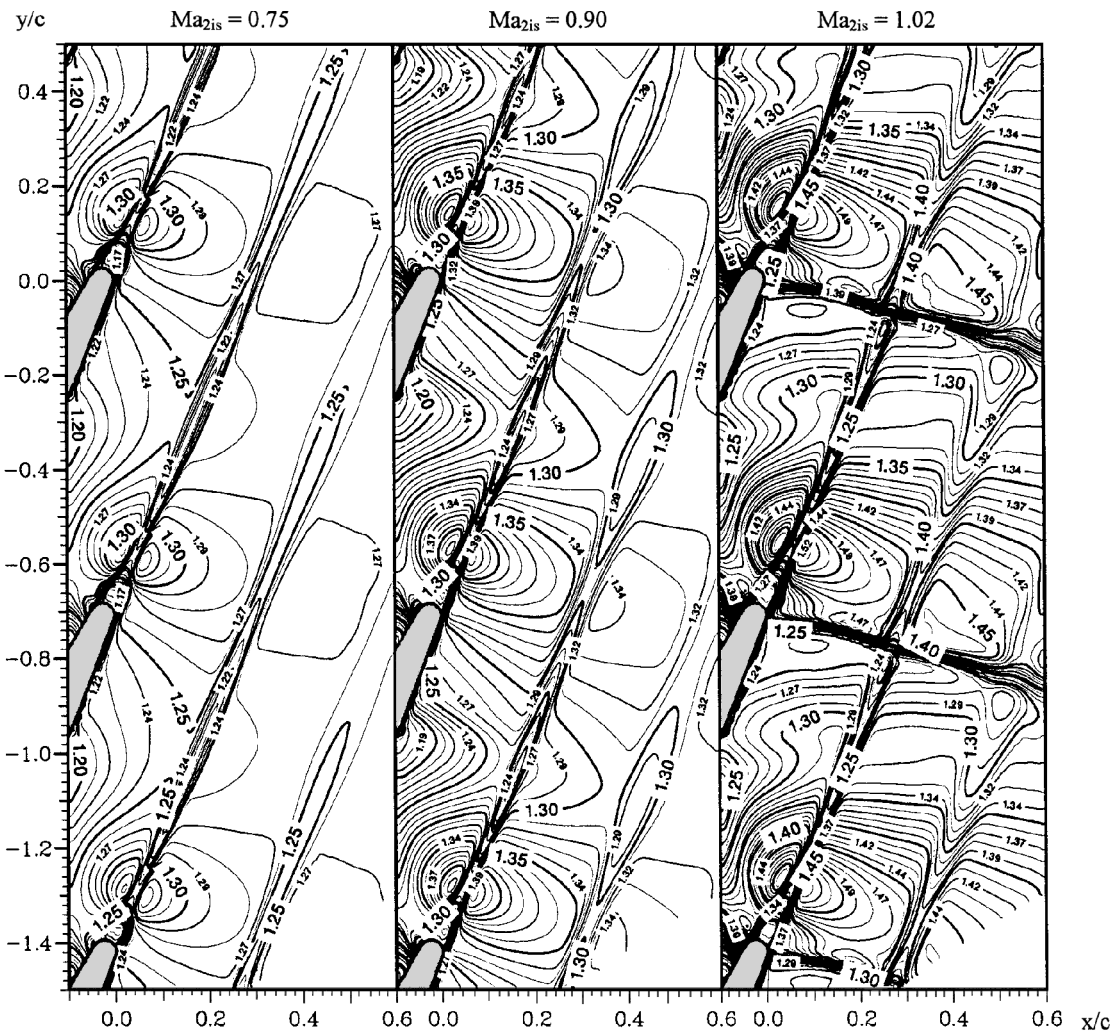

Fig. 7 Calculated density fields.

expansion ratios as needed, e.g., for transonic flow. The water particles cause extreme scattering, which falsifies the results or, in the worst case, prevents evaluation due to local saturation on the CCD chip. Because of this, the outlet Mach number in all experiments was chosen sufficiently low so that condensation could not occur, depending on the humidity of the ambient air and on the inlet temperature level. Thus, the highest achievable Mach number in summer was $Ma_{2is} = 0.75$, and it was $Ma_{2is} = 1.05$ on cold dry winter days. Even though the air is led through a dust filter, a few small particles may reach the measuring area. But it is ensured that there are fewer particles effecting Mie scattering than the limit Schweiger[8] established for neglecting Mie scattering in Rayleigh experiments.

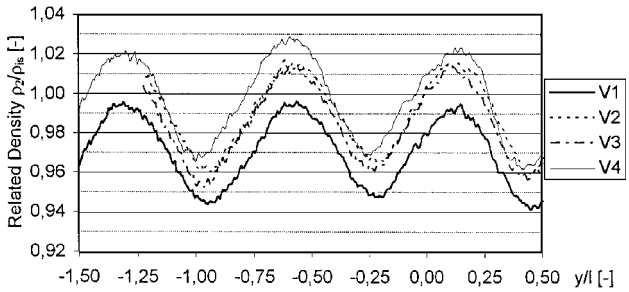

Fig. 8 Related densities at $x/\ell = 0.2$ from different measurements, $Ma_{2is} = 0.75$.

Results

Figure 6 shows the results from three different Rayleigh scattering experiments ($Ma_{2is} = 0.75$, 0.90, and 1.02) with an increment of 0.01 kg/m^3; Fig. 7 shows the corresponding numerical results. The density fields were calculated with a simulation program, using Navier–Stokes equations with the Baldwin–Lomax turbulence model.[9]

The density fields of the three measured flow channels are almost identical. The nonperiodicities between the flow channels are hardly noticeable; they are caused by small manufacturing inaccuracies of the cascade. As can be seen, usable Rayleigh scattering signals can be recorded even at $Ma_{2is} = 0.75$, although the density variations amount to only 4–12%, according to the density of the ambient air.

To determine the reproducibility, additional measurements were accomplished at $Ma_{2is} = 0.75$, within a time range of four months. Before each testing, the optical setup was adjusted to avoid systematic errors of the setup. Figure 8 shows the density distributions at $x/\ell = 0.2$ related to the isentropic outlet density. The densities deviate only within a maximum $\pm$1.5%, and so a very good reproducibility can be found. This uncertainty in reproducibility of 1.5% includes the aforementioned sources of error such as energy monitoring or the camera system and the uncertainty of determining ρ_0.

On the suction sides near the trailing edges, strong density gradients already can be seen at subsonic flow. At $Ma_{2is} = 1.02$, a shock

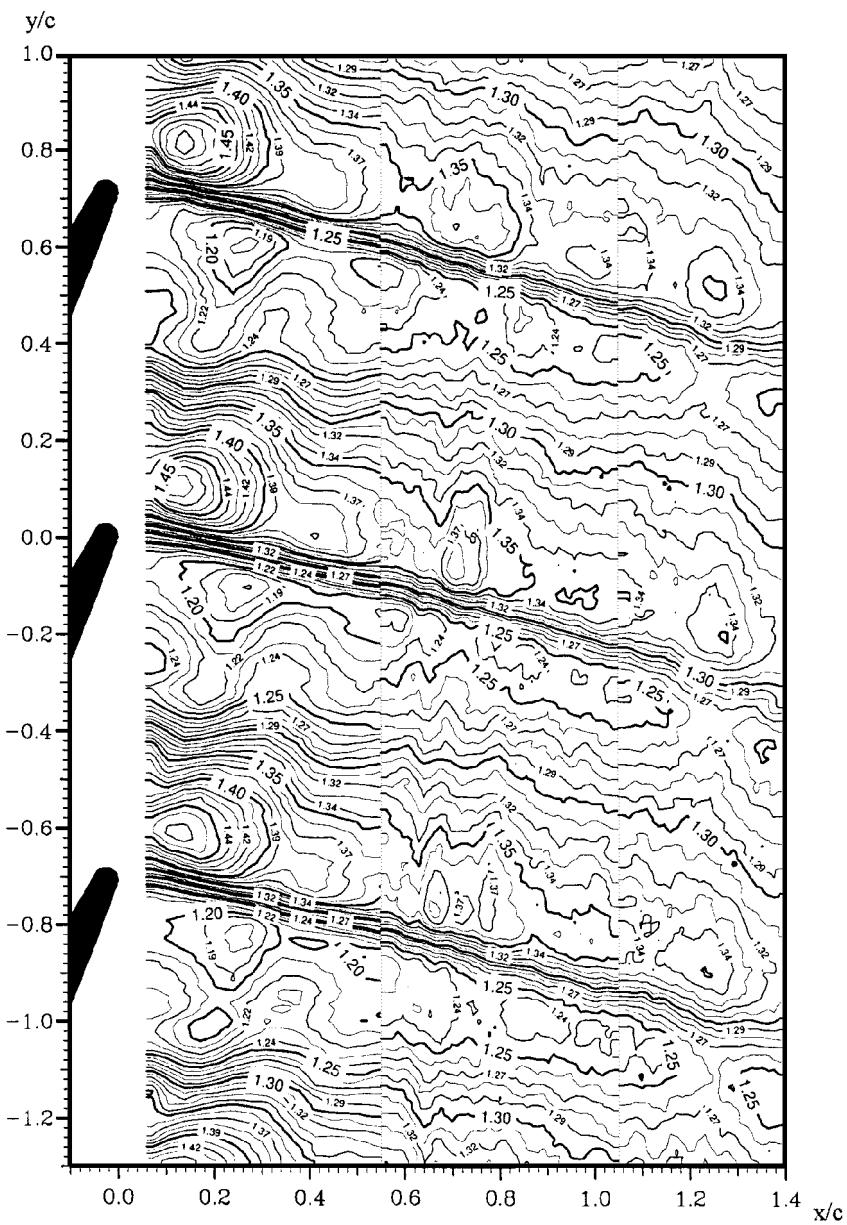

Fig. 9 Measured density fields at $Ma_{2is} = 1.05$.

wave can be recognized with a nature that is typical for transonic turbine cascades. The shock wave crosses the wake and barely widens up to the end of the evaluation area at $x/\ell = 0.6$.

All computational results show qualitatively distinctive and spatial restricted wakes that cannot be proved true by the experiments. Comparable calculations with different grids yield a strong dependence of the computed wake structure on the number of grid points in this area of interest.[6] The number of grid points in the wake has no influence on the calculated surface Mach numbers. The differences described here might be caused by an inadequate modeling of the mixing of wake and isentropic flow in the program being used. Also, another program, which we had at our disposal, yields these spatial restricted wakes even more markedly. A qualitatively good agreement of measurement and calculation can be seen outside the wakes.

Nevertheless, the measured density isolines, starting on the suction side near the trailing edges, develop a little more flatly than the computational ones. In particular, at transonic flow the measured and the calculated shock waves show an angle difference of about 8 deg.

The quantitative comparison yields about 1–2% higher density values at the simulation. This might be caused either by somewhat lower calculated losses or by the boundary conditions not fitting all parameters.

Based on these results, an investigation was conducted to determine whether density information can be received from a very much enlarged section of the outlet flowfield with the help of compositing single images. For this, three measurements were accomplished at identical flow conditions but with different distances between the laser beam and the trailing edges. The recorded images were evaluated and put together on one contour plot, which reached from $x/\ell = 0.06$ to 1.40. The isentropic outlet Mach number was chosen as $Ma_{2is} = 1.05$ because then effective density gradients could be expected even far from the trailing edges. The result is shown in Fig. 9.

It clearly can be seen that these three single density fields qualitatively fit together very well. As expected, the lines of constant density form common structures across the borders of the single-image planes. This can be seen especially at the shock waves because there are no alterations of the wave courses and dimensions at the separation lines. Quantitatively small level differences can be determined between the single measurements, but these variations are within the scope of the already discussed experiment uncertainty. They may be caused by the uncertainty of the energy monitoring.

Comparing the results of $Ma_{2is} = 1.05$ with $Ma_{2is} = 1.02$, the following differences are conspicuous. At higher outlet Mach numbers, the starting point of the shock wave shifts in flow direction and the wave course is tipped with an angle of +6 deg. At $Ma_{2is} = 1.05$, the wave is clearly distinguishable almost until the edge of the measuring area at $x/\ell = 1.4$. These characteristics for increasing Mach number are typical for the VKI-1 cascade and were proved qualitatively by experiments[10,11] and calculations.[12]

Conclusions

The measuring system described here allows a two-dimensional quantitative density field to be recorded with very good reproducibility in a few seconds. Variations in air density of less than 1% are distinguishable. The measurements are accomplished without disturbing the flowfield because the measuring system needs neither probes in the test section nor tracer particles for light scattering. The results show that it is possible to expand the measuring area as much as desired with the help of compositing single measured images. At present, preparations are being made for measurements of the density distribution from several planes with different distances to the endwalls. After adjusting and optimizing the experimental arrangement, the density field between the blades also will be measured. These investigations will yield the complete three-dimensional quantitative density field inside and behind the turbine cascade.

References

[1]Escoda, M. C., and Long, M. B., "Rayleigh Scattering Measurements of the Gas Concentration Field in Turbulent Jets," *AIAA Journal*, Vol. 21, No. 1, 1983, pp. 81–84.

[2]Smith, M., Smits, A., and Miles, R., "Compressible Boundary-Layer Density Cross Sections by UV Rayleigh Scattering," *Optics Letters*, Vol. 14, No. 17, 1989, pp. 916–918.

[3]Miles, R., and Lempert, W., "Two-Dimensional Measurement of Density, Velocity and Temperature in Turbulent High-Speed Air Flows by UV Rayleigh Scattering," *Applied Physics B*, Vol. 51, July 1990, pp. 1–7.

[4]Shimizu, H., Lee, A., and She, C. Y., "High Spectral Resolution Lidar System with Atomic Blocking Filters for Measuring Atmospheric Parameters," *Applied Optics*, Vol. 22, No. 9, 1983, pp. 1373–1381.

[5]Sieverding, C. H., "The Turbine Blade Definition," *Transonic Flows in Turbomachinery*, Lecture Series 59, von Kármán Inst. for Fluid Dynamics, Rhode Saint Genèse, Belgium, 1973.

[6]Sieber, O., "Quantitative Dichtefeldmessung mit Rayleigh-Streulicht am Laufschaufelprofil VKI-1 und Vergleich mit einer numerischen Simulation," Vol. 301, *Fortschrittsberichte VDI Reihe 7*, VDI-Verlag, Düsseldorf, Germany, 1996.

[7]Allen, C. W., *Astrophysical Quantities*, Athlone, London, 1973, Chap. 6.

[8]Schweiger, G., "Lokale Dichtemessung in verdünnten Gasen mit Hilfe der Laserlichtstreuung," Deutsche Forschungs- und Versuchsanstalt für Luft- und Raumfahrt, Forschungsbericht 73-83, Porz-Wahn, Germany, 1973.

[9]Schöll, E., "Ein dreidimensionales Rechenverfahren für reibungsbehaftete Strömungen in Schaufelreihen von Turbomaschinen," Vol. 287, *Fortschrittsberichte VDI Reihe 7*, VDI-Verlag, Düsseldorf, Germany, 1996.

[10]Lehthaus, F., "Experimentelle Untersuchungen an einem Gasturbinen-Laufrad-Gitter mit dem Schaufelprofil VKI-1, Teil 1: Messungen im Abströmfeld und Schlierenaufnahmen," Deutsche Forschungs- und Versuchsanstalt für Luft- und Raumfahrt, Rept. 251 74 A 48, Göttingen, Germany, Jan. 1975.

[11]Sieverding, C. H., "Experimental Data on Transonic Turbine Blade Sections and Comparison with Various Theoretical Methods," *Transonic Flows in Turbomachinery*, Lecture Series 59, von Kármán Inst. for Fluid Dynamics, Rhode Saint Genèse, Belgium, 1973.

[12]Arnone, A., and Swanson, R. C., "A Navier–Stokes Solver for Turbomachinery Applications," *Journal of Turbomachinery*, Vol. 115, April 1993, pp. 305–313.

G. Laufer
Associate Editor